THE HOMOGENEITY OF SPHEROIDAL POPULATIONS IN DISTANT CLUSTERS*

Richard S. Ellis[1], Ian Smail [2†], Alan Dressler[3], Warrick J. Couch[4],
Augustus Oemler Jr.[5‡], Harvey Butcher[6] & Ray M. Sharples[2],
1) Institute of Astronomy, Madingley Rd, Cambridge CB3 OHA, UK
2) Department of Physics, University of Durham, South Rd, Durham DH1 3LE, UK
3) The Observatories of the Carnegie Institution of Washington, 813 Santa Barbara St., Pasadena, CA 91101-1292
4) School of Physics, University of New South Wales, Sydney 2052, Australia
5) Astronomy Department, Yale University, PO Box 208101, New Haven CT 06520-8101
6) NFRA, PO Box 2, NL-7990, AA Dwingeloo, The Netherlands

ABSTRACT

The small scatter observed for the $(U-V)$ colors of spheroidal galaxies in nearby clusters of galaxies provides a powerful constraint on the history of star formation in dense environments. However, with local data alone, it is not possible to separate models where galaxies assembled synchronously over redshifts $0 < z < 1$ from ones where galaxies formed stochastically at much earlier times. Here we attempt to resolve this ambiguity via high precision rest-frame UV–optical photometry of a large sample of morphologically-selected spheroidal galaxies in three $z \sim 0.54$ clusters which have been observed with HST. We demonstrate the robustness of using HST to conduct the morphological separation of spheroidal and disk galaxies at this redshift and use our new data to repeat the analysis conducted locally at a significant look-back time. We find a small scatter (< 0.1 mag rms) for galaxies classed as Es and E/S0s, both internally within each of the three clusters and externally from cluster to cluster. We do not find any trend for the scatter to increase with decreasing luminosity down to $L \sim L_V^* + 3$, other than can be accounted for by observational error. Neither is there evidence for a distinction between the scatter observed for galaxies classified as ellipticals and S0. Our result provides a new constraint on the star formation history of cluster spheroidals prior to $z \simeq 0.5$ confirming and considerably strengthening the earlier conclusions. Most of the star formation in the elliptical galaxies in dense clusters was completed before $z \simeq 3$ in conventional cosmologies. Although we cannot rule out the continued production of *some* ellipticals, our results do indicate an era of initial star formation consistent with the population of star-forming galaxies recently detected beyond $z \simeq 3$.

Subject headings: cosmology: observations – galaxies: evolution – galaxies: photometry – clusters of galaxies

Received -_____; accepted -_____

---

* Based on observations obtained with the NASA/ESA Hubble Space Telescope which is operated by STSCI for the Association of Universities for Research in Astronomy, Inc., under NASA contract NAS5-26555.

†Visiting Research Associate at the Carnegie Observatories.

‡Present address: The Observatories of the Carnegie Institution of Washington, 813 Santa Barbara St., Pasadena, CA 91101-1292

1. Introduction

Elliptical galaxies are conventionally regarded as old galactic systems whose star formation history can be approximated as a single burst that occurred 12–16 Gyr ago (Baade 1958; Tinsley & Gunn 1976; Bruzual 1983). However, in recent years, this simple picture has been subjected to a number of challenges. Numerous cases have been found of ellipticals with intermediate-age stellar populations (O'Connell 1980) and dynamical arguments suggest that many peculiarities seen in ellipticals (shells and dust-lanes) are best explained via recent formation from the merger of gas-rich systems (Toomre 1978; Quinn 1984). Detailed spectroscopy of such systems provides a rich set of data whose interpretation in terms of star formation history requires an adequate separation of the competing effects of metallicity and age (Worthey 1995).

The conflict might be resolved if the majority of ellipticals were old single burst systems, whereas the remainder formed via merging of gas-rich disk galaxies. In this case one might expect an environmental and/or mass dependence in the rate of occurrence of intermediate age populations. Reasonably good evidence is emerging that recent star formation is more prevalent in low density environments than in clusters. Rose et al. (1994) find the mean stellar dwarf/giant ratio is higher in environments with low virial temperatures. This would be consistent with other environmental trends which indicate accelerated star formation histories in clusters (Oemler 1991).

Sandage & Visvanathan (1978) first proposed that the UV-optical color-magnitude (C-M) relation for cluster galaxies could provide a significant constraint on their past history of star formation. The improved precision possible with modern CCD detectors was exploited by Bower, Lucey & Ellis (1992, hereafter BLE) who obtained high precision U and V photometry of spheroidal galaxies in two local clusters, Virgo and Coma. BLE observed a very small scatter, $\delta(U-V)\lesssim 0.035$, around the mean color-luminosity relation for luminous E/S0's, which was barely larger than that attributable to observational errors.

The sensitivity of the U-band light to small numbers of hot, young stars enabled BLE to constrain the past contribution from upper main sequence stars statistically across both cluster samples. With a single present-day value for the scatter they chose to express their result in a number of ways. Firstly, in terms of the passive evolution of a single-burst population, the tightness of the C-M relation was used to derive a minimum age. In the absence of any recent star-formation, the homogeneity of the Virgo and Coma populations would suggest stochastic formation of galaxies could only occur within the first few Gyr after the big bang (i.e. $z>2$ in cosmologies with H_o=50 and Ω=0.1). Unfortunately, such absolute age estimates are subject to many of the uncertainties which afflict those for globular clusters.

More convincingly, abandoning the constraint on the age of the first burst, BLE also concluded that no more than 10% of the current stellar population in present-day E/S0s could have been formed in any subsequent activity in the past 5 Gyr as might be the case if merging of gas-rich systems had been involved. They expressed this result more generally in terms of a combined synchronicity+age constraint. Recent activity from major merging would only be consistent with the tight $(U-V)$ scatter if the star formation history had been similar from galaxy to galaxy both within each cluster and between the Coma and Virgo clusters.

BLE's result presents an important challenge for bottom-up hierarchical theories of structure since these predict relatively recent formation eras for massive galaxies. Baugh et al. (1996) and Kauffmann (1996) have addressed the question quantitatively using a simple prescription for merger-induced star formation. They find that the homogeneity of BLE's C-M data can be satisfied if the merging of disk galaxies that produce the spheroidals was largely complete by a redshift $z\simeq 0.5$.

Although good progress has been made in tracking the UV-optical C-M relation to higher redshift (Ellis et al. 1985; Aragón-Salamanca et al. 1991, 1993), without morphological information a major uncertainty

remains. The scatter of the photometric C-M relation may be underestimated if some spheroidal galaxies lie blueward of the C-M sequence. This could well be the case if the timescale for dynamical evolution is shorter than that for main sequence evolution as indicated in numerical simulations (Mihos 1995; Barger et al. 1996a). This point was originally examined by MacLaren et al. (1988) who showed that a detectable UV excess could remain for $\simeq$2 Gyr *after* a burst induced, for example, by a merger.

In this paper, we extend the analysis of BLE to a sample of three $z \simeq 0.54$ clusters, taking advantage of images from the *Hubble Space Telescope* (HST) Wide Field Planetary Camera 2 (WFPC-2) to morphologically classify a sample of faint galaxies. In §2 we summarise the new observations and describe our photometric techniques and morphological classifications. A key question we examine is the reliability of using HST to isolate distant spheroidals. In §3 we discuss the color-magnitude relationships, both absolutely in terms of predictions for no evolution and in terms of the photometric scatter. §4 discusses the main result in the context of the star formation history of cluster galaxies and explores the likely consequences in terms of locating the epoch of their formation. §5 summarises our principal conclusions.

2. Data

2.1. Observations

The observations presented here consist of deep F555W and F814W images of the core regions of three $z \simeq 0.54$ clusters obtained using the WFPC-2 (Figure 1). The data form part of a larger study of the morphologies of galaxies in distant clusters (the "MORPHS" project – Smail et al. 1996a,b (S96); Dressler et al. 1996, 1997; Barger et al. 1996b). The clusters discussed here cover a range of optical richnesses and X-ray luminosities within a narrow redshift interval specifically selected so that observed F555W/F814W is close to rest-frame U/V. At $z = 0.54$ the F555W passband (525 ± 61 nm) samples 341 ± 40 in the restframe with F814W (828 ± 88 nm) lying at 538 ± 57 nm, compared to U and V at 365 ± 70 nm and 550 ± 90 nm respectively. Using these passbands we can thus analyse our cluster data in a similar way to BLE, the principal difference being the significant look-back time. In order of decreasing mass or X-ray luminosity, the clusters are Cl0016+16 at $z = 0.546$ (Koo 1981; Ellis et al. 1985; Dressler & Gunn 1992; Aragón-Salamanca et al. 1993), Cl0054−27 at $z = 0.563$ (Couch et al. 1985, 1991) and Cl0412−65 ($\equiv F1557.19TC$) at $z = 0.510$ (Couch et al. 1991; Bower et al. 1994, 1996). Further properties of these systems and a log of the HST observations are given in Table 1.

The individual exposures in each passband are grouped in 2 sets, each offset by 2 arcsec to allow hot pixel rejection. After standard pipeline reduction, the images were aligned using integer pixel shifts and then combined into final F555W/F814W frames using the IRAF/STSDAS task CRREJ. We chose to work in the WFPC-2 filter system (which we call V_{555} and I_{814}), calibrated from our own ground-based images of the clusters using the color transformations given in Holtzman et al. (1995), as discussed below. The final images (Figure 1) cover the central 0.7 h^{-1} Mpc,[§] i.e. ~ 0.35 h^{-1} kpc/pixel. The processed data reaches a 5σ limiting depth of $I_{814} = 26.7$ and provides $(V_{555} - I_{814})$ colors with better than 2% precision at $I_{814} = 21.0$ and 5% at the limit of $I_{814} = 23.0$ used in this analysis (see below).

[§]Unless otherwise stated, we use $q_o = 0.5$ and $h = H_o/100$ km sec^{-1} Mpc^{-1}. Thus 1 arcsec $\equiv$3.6 h^{-1} kpc (Cl0412−65) or 3.7 h^{-1} kpc (Cl0016+16, Cl0054−27)

As we will compare this analysis with BLE's previous study of early-type galaxies in the Coma and Virgo clusters, it is important to consider the physical regions of the clusters sampled as well as the spatial resolution and photometric precision of the relevant ground-based and HST datasets. In the case of BLE, galaxies were selected according to the availability of stellar velocity dispersions from Dressler (1984); generally they lie within 500 h^{-1} kpc of the cluster centre. BLE's analysis was based on aperture photometry within a diameter $\simeq 5h^{-1}$ kpc (60 arcsec at Virgo, 11 arcsec at Coma). Over a total luminosity range of $\simeq$4 mags to a limiting absolute magnitude of $M_V \simeq -17 + 5\log h$, the rms photometric error in $(U-V)$ was 0.03 mag. As we will see below, we can reproduce these quantities fairly closely with the HST samples.

2.2. Reduction and Photometric Precision

We selected galaxies in the HST frames from the stacked F814W (restframe $\sim V$) images using the SExtractor package of Bertin & Arnouts (1996). After convolving the data with a top-hat kernel of diameter 0.3 arcsec, all objects with areas greater than 12 pixels above the $\mu_{814} = 25.0$ mag arcsec^{-2} isophote were evaluated. This ensures a source list which extends much fainter than that eventually used in this analysis. Color were measured using an aperture with a diameter of 5 h^{-1} kpc ($\sim$ 1.4 arcsec) closely matching that used by BLE and total magnitudes were obtained from the SExtractor **BEST_MAG** estimates. We discuss the precision of both the aperture and integrated photometry next.

2.3. Calibration of $(V_{555}-I_{814})$ between clusters

An important aim of our investigation is to not only examine the scatter *internal* to each cluster but also *externally* across the three clusters. This requires precise relative colors between the three clusters and we have thus chosen to independently determine the photometric zero-points of our WFPC-2 images using ground-based images of the HST fields, rather than having to assume that our various WFPC-2 F555W/F814W observations have fixed zero-points. The ground-based data were all obtained on a single photometric night and thus provide a robust calibration of the colors of galaxies across the three clusters. The images were kindly provided by Barry Madore and were taken using a thinned 2k^2 Tek CCD on the 2.5m Du Pont telescope at Las Campanas Observatory (LCO), Chile. The clusters were observed in Johnson V and Cousins I across a range in airmasses, 1.2–1.5, on the night of October 14th, 1996. A large number of Landolt (1992) standard fields were also observed during this time, bracketing the airmass range of our observations. The total integrations on our clusters are 500s in V and 800s in I, with seeing of FWHM=1.0–1.2 arcsec. These data were reduced and calibrated in a standard manner using dome and sky flats. Analysis of the standard fields shows that the night was photometric and allows us to derive extinction and color calibration of our science observations to an accuracy of $\pm$0.029 in V and $\pm$0.015 in I, where we include the uncertainty for extrapolating the color correction from the range of our standard stars $(V-I) \sim 1$ to the expected colors of E/S0's in the distant clusters $(V-I) \sim 2.5$.

We next measure photometry within 3 arcsec diameter apertures from these V and I images, having matched the seeing in the frames from measurements of the stellar profiles. To reduce our sensitivity to residual color corrections we have chosen to restrict our comparison to just those red E/S0 galaxies from our HST images which are used in the analysis below. We also apply a further magnitude limit to this

sample owing to the shallower depth of our ground-based images, hence we restrict ourselves to galaxies with $I \leq 20.5$. Having measured the colors of these galaxies on the ground-based images we convert our $(V-I)$ to $(V_{555}-I_{814})$ using the color equations given for the WFPC-2 flight system in Table 7 of Holtzman et al. (1995). We can now compare this photometry with that obtained from our WFPC-2 images, where we have assumed a single zero-point for the F555W and F814W images of the three clusters. We determine offsets in the zero-points of the WFPC-2 photometry relative to the LCO data of -0.017 ± 0.035, -0.062 ± 0.043 and 0.072 ± 0.036 for Cl0016+16, Cl0054−27 and Cl0412−65, where the errors in the means are estimated by bootstrap resampling. While using a single WFPC-2 zero point would be accurate in the mean: -0.002 ± 0.068, the scatter between the clusters (especially for Cl0412−65) justifies our recalibration. Having applied these corrections to our photometry we now have a robust calibration of $(V_{555}-I_{814})$ across our three clusters with a precision of 4%.

2.4. Calibration of $(V_{555}-I_{814})$ between WFC CCDs

We have also tested the relative photometry across the WFPC-2 field to estimate contributions to the scatter of the entire sample from possible zero-point variations between the CCD chips. Unfortunately, the calibrations shown above lack sufficient numbers of objects to allow us to undertake this test for all three clusters. However, we can apply this with adequate precision by comparing our HST photometry with deep high resolution ground-based images of a single cluster, Cl0016+16 (Smail 1993; Smail et al. 1994), to search for systematic offsets as a function of position. Here we are searching for a variation in the difference between the colors of galaxies measured on the ground-based image and the three WFC CCDs. Owing to the slightly different color responses of the ground-based Johnson V and Cousins I compared to F555W and F814W we compare photometry only for those objects which lie in a relatively narrow band in the HST color-magnitude diagrams. To $I_{814}<23.0$ we have ~ 230 galaxies across the three chips. We set a firm upper limit of $\Delta = 0.02$ mag on the relative offsets in $(V_{555}-I_{814})$ between the chips.

2.5. Photometric precision

The photometric errors on our HST aperture magnitudes have been estimated by analysing both the variance in the background sky and the poisson noise in the object counts. We have confirmed the estimates so obtained by splitting the imaging data for one of the clusters (Cl0016+16) into two independent sets and comparing the photometry of 160 of the $I_{814}<23.0$ objects measured off each half. For $I_{814}=22.0$ we find an average photometric error in $(V_{555}-I_{814})$ of ± 0.016 increasing to ± 0.063 at $I_{814}= 23.0$; the median values are ± 0.015 and ± 0.053 respectively. The distribution of the differences for the two independent datasets in Cl0016+16, when scaled by the theoretical uncertainties shows a distribution consistent with these errors. The typical difference in integrated I_{814} magnitudes from the SExtractor photometry of the Las Campanas and WFPC-2 images of the spheroidal galaxies in the three clusters is $(I_{814}^{\rm HST} - I_{814}^{\rm LCO}) \simeq 0.1$ mag at $I_{814} \simeq 21.0$. Examining the variance in the profile fits, we also estimate an uncertainty of ± 0.1 mag in the total magnitudes adopted.

We will generally consider three magnitude-limited samples for each of our clusters. The brightest sample is limited at $I_{814} < 21.0$ corresponding to an absolute magnitude of $M_V \simeq -19.8 + 5 \log h$ $(L_V \sim L^* + 1)$. At this limit the morphological distinction between Es and S0s is relatively clear, although

we discuss below the level of mixing between these two samples due to misclassification. To I_{814}= 22.0, a large fraction of the galaxies are spectroscopic-confirmed members and the photometric precision is similar to that obtained by BLE. The faintest sample is limited at I_{814}< 23.0 – or $M_V < -17.8 + 5\log h$ – and enables us to investigate the possibility of a variation in the $(V_{555}-I_{814})$ scatter along the cluster C-M relation for the spheroidal (E and S0) population as a whole.

Finally, we compare the precision of the photometry available from our HST images and the 4.2m William Herschel Telescope (Smail 1993; Smail et al. 1994) for Cl0016+16. At the faintest limit of our classifications, I_{814}=23.0, the HST rms error on $(V_{555}-I_{814})$ is 70% of that obtained from the larger aperture WHT, despite good conditions and longer integrations. This can be understood in terms of the reduced sky background at longer wavelengths. Specifically, the I_{814} sky is $\simeq$8 times fainter in space and this gain is equivalent to an effective aperture increase of $\simeq \times 2.6$ for background-limited work. Thus HST has significant photometric advantages at faint limits quite apart from its superior image quality.

2.6. Photometric Corrections

Before analysing the C-M relations and the associated UV–optical scatter, it is important to introduce two further small corrections that must be made to the galaxy photometry if we wish to combine the data across all three clusters.

Firstly, we have taken the interstellar reddening for our three fields from the NED database.[¶] We find A_B = 0.08, 0.06 and 0.10 for Cl0016+16, Cl0054−27 and Cl0412−65 respectively. As these effects are differentially very small, we will apply corrections only to the $(V_{555}-I_{814})$ colours using the conversion $\delta\,(V_{555}-I_{814})= 0.36\ A_B$ and reducing all colors to those appropriate for Cl0016+16. The corrections involved are small (<0.007).

Secondly, a small correction must be made to allow for the relative k-correction difference across the three clusters, which have slightly different redshifts. This can be done most simply by adopting a spectral energy distribution (SED) and taking the derivative $\delta\,k(V_{555}-I_{814})/\delta\,z$ at the mean cluster redshift $\overline{z}$=0.54. Adopting the SED of a present-day giant elliptical with $M_V \simeq -19.8 + 5\log h$ ($I_{814} \sim 21$ at $z = 0.54$) (Aragón-Salamanca et al. 1993) gives $\delta\,k(V_{555}-I_{814})\ /\ \delta\,z$=1.8 and thus the differential color shift is found to be <0.05 mag.

As the slope of the C-M relation is relatively constant with redshift (see below), provided data is compared from one cluster to another at the same luminosity, the second-order effect to the redshift correction arising from SED variations with luminosity is very small. This was examined by interpolating to the SED of a present-day Sab galaxy (c.f. techniques discussed in Couch et al. 1984) where we found a negligible difference in the differential color term (<0.01).

Combining both reddening and redshift effects, the color corrections we have applied are −0.025 and 0.057 for Cl0054−27 and Cl0412−65, respectively.

2.7. Morphological Classification

[¶]NED (the NASA/IPAC Extragalactic Database) is operated by the Jet Propulsion Laboratory, California Institute of Technology, under contract with the National Aeronautics and Space Administration.

A central issue to an application of the BLE technique at $z \simeq 0.54$ is the separation between disk and spheroidal galaxies from the HST images. In this section we describe our classification methods and various tests conducted to test the reliability of our results.

The morphological classifications for the various samples in each of the three clusters were first determined independently by three of us (AD/WJC/RSE) and subsequently combined into a single class according to a scheme we have defined as part of the larger project to study the evolution of galaxies in our cluster sample (S96). The images were classified blind according to a list with no regard to either the spectroscopic or color data. More extensive details of the classification scheme and its precision are given in our catalog paper (S96). Here we are primarily concerned with the accurate selection of the spheroidal population and the precision with which the E and S0 subclasses can be identified to various depths. In our classifications we use the term 'E/S0' to describe an ambiguous case, E or S0, rather than to classify actual transition cases (in this we differ from the approach used in the Revised Hubble scheme).

The suitability of ≃3-6 orbit WFPC-2 data (shallower than that used here) for the morphological classification of distant galaxies has been addressed by Glazebrook et al. (1995) and Abraham et al. (1996a) by simulating the appearance of $z \simeq 0.7$ galaxies in the F814W band using nearby CCD data. Those studies carefully take into account the various detector and imaging point spread functions and, in the case of Abraham et al. (1996b), accurately allow for k-correction losses on a pixel-by-pixel basis using spectral energy distributions assigned from multicolor data. Those workers found that misclassifications generally only become significant beyond $z \simeq 1$ and then mostly for intermediate and late-type spirals. The combination of the differential k-correction between disk and bulge light and surface brightness losses imply a shift to apparently later types.

In this study a key question is the reliability of isolating the boundary between early-type spirals and S0s as well as the distinction between Es and S0s, which is troublesome even at low redshift. One worry is that, even over a smaller range in redshift for which the differential k-correction effect is small, surface brightness losses may make certain early spirals appear more bulge-dominated. That such effects are unlikely to be significant is illustrated by Figure 2 (kindly prepared by Roberto Abraham) which presents a mosaic of representative present-day elliptical, S0 and Sa galaxies taken from the catalog of Frei et al. (1996) simulated as they would appear in the F814W band at z=0.5 taking into account all the various HST-specific factors discussed above. Clearly, the majority of the diagnostic features used to differentiate these systems locally remain clearly visible.

Turning to the cluster images, Figure 3 illustrates both the ease with which the classifications can be made to various limits as well as highlighting some difficult cases we encountered. Where possible we have chosen spectroscopically confirmed members. A comparison of the morphological classifications of the three classifiers is our primary guide since we wish the classifications to be strictly independent of color and spectroscopic properties.

To I_{814}=21.0 across all Hubble types, the morphological types on a scheme of 10 classes (S96) are in unanimous agreement for the three classifiers for 70% of the galaxies and within ±1 type for all objects (S96). Most significantly for this study, 86% of the ellipticals and 60% of the S0s to I_{814}=21.0 were unanimously chosen as such by all three classifiers. Examples of these objects are contained in the top two rows of Figure 3. Note that, in calculating this success rate, instances where one classifier indicated 'E/S0' have been rejected. Together with Abraham's simulations, this suggests the morphological types to I_{814}=21.0 are as good as those in the local clusters, in particular for discriminating between spheroidals and disk galaxies.

From I_{814}=21.0 to 23.0 the overall agreement across the Hubble sequence worsens as might be expected. Examples of these galaxies are shown in the third row of Figure 3. Unanimous agreement

amongst the three classifiers across all types falls from 70% to 40% with about 90% of the objects being classed to within ±1 type (previously 100%). Fortunately, this does not impact significantly on the precision with which ellipticals can be identified. 70% of the classed Es were chosen definitely as such by all three classifiers. However only 25% of the S0s were similarly identified.

The issue of misclassification of round E and S0 galaxies is dicussed in detail in S96, but we review it here briefly owing to its importance for this analysis. Discriminating between E and face-on S0 galaxies has always been a concern for morphological classification. A crude estimate of the proportion of misclassified face-on S0s can be made from the observed ellipticity distribution of S0s, under the assumption that they can be simply modelled as randomly-projected thin disks. Such a model predicts a flat distribution of numbers of S0's with ellipticity, when compared to this the observed fraction of S0s provides an estimate on the likely misclassification rate. Looking at the fraction of S0s with $\epsilon \leq 0.3$ we find $23 \pm 10\%$ to I_{814}=23 in the three clusters. Compared to the expected fraction of 33% (S96) this indicates that we maybe misclassifying up to 10% of the S0 population. When combining all the data from our three clusters (22 S0 galaxies) this amounts to 2–3 galaxies in total (compared to 60-or-so ellipticals) and so it is difficult to see how it might strongly affect our results. We will incorporate this estimate into our analysis below, as well as other possible sources of morphological contamination.

Finally, in addition to the visual classification, we investigated a more quantitative approach based on surface photometry profiles from the HST images. We considered this might be helpful in addressing the possibility that some bulge-dominated systems with faint disks may be misclassified as ellipticals. We examined surface brightness profiles for 12 cases with I_{814}=21.0–22.0 where there was some disagreement between the morphological classifiers. For five galaxies convincingly identified to be ellipticals on the basis of profiles, four had been identified as such morphologically by two of the three classifiers but the third disputing classifier led to our being cautious and assigning E/S0 in two cases. Only one profile-classed elliptical was thought morphologically to be a S0. Likewise, two disk galaxies identified from profiles had been assigned E/S0 on the basis of the morphologies suggesting a similar effect. For the remaining five cases where there was disagreement between the morphologists, the profile data was inconclusive. The results suggest that whilst there is no major discrepancy between the two approaches to classification, the surface brightness profiles are not particularly helpful in deciding in cases of difficulty.

In summary therefore, the morphological selection of spheroidal galaxies appears reliable to the limit of our sample. However, the distinction between E and S0 becomes somewhat uncertain fainter than I_{814}=21.0–22.0 and may result in upto 10% of our S0s being misclassified as E.

3. Analysis

3.1. Estimating the Field Contamination

It is important at this stage to consider the possibility of contamination of the cluster data from field galaxies, especially any that might be morphologically early-type galaxies. First we discuss the limited spectroscopic data that is available for our clusters.

Cl0016+16 has been studied by Dressler and Gunn (1992) and also, more recently, by the CNOC group (Carlberg et al. 1996) who have kindly made their results available to the authors (Abraham, private communication). Excluding stars, the original Dressler and Gunn spectroscopy provides redshifts for 31 galaxies in the WFPC-2 field of which 7 are non-members. The CNOC group observed 14 galaxies in the

same area of which 8 have redshifts in close agreement with Dressler and Gunn; 6 are new redshifts and all are cluster members. Examining the 7 non-members, the redshifts cover a wide range and none are morphologically spheroidal galaxies. The foreground group at z=0.30 suggested by Ellis et al. (1985) on the basis of their SED fitting does not feature as prominently as those authors had suggested. Only three galaxies have redshifts associated with this structure.

In Cl0412−65, spectra are available for our new study (Dressler et al. 1997) for 4 new members and a further 4 non-members. In addition spectra exist for 13 more galaxies from the recent study of Bower et al. (1996) of which 5 are non-members. Amongst the 9 spectroscopically-confirmed field galaxies, none was classed as spheroidals and thus no correction for contamination can be made on this basis. For Cl0054−27 spectroscopy is published for only the two brightest members (Couch et al. 1985) and we supplement this with new data on a further 10 members and 4 non-members from Dressler et al. (1997). Again there were no field spheroidals identified.

Overall, the spectroscopic coverage is sufficiently poor, that field contamination must therefore be evaluated statistically. Glazebrook et al. (1995) and Abraham et al. (1996b) present the morphologically-dependent counts from the HST Medium Deep Survey and as one of us (RSE) was involved in the classification of that sample, it is well suited for estimating the number of field E/S0s in each cluster field as well as their color distribution. As the MDS data has only been classed to I_{814}=22.0, we have also taken the deeper classifications of Driver et al. (1995) as well as counts from the Hubble Deep Field (Abraham et al. 1996a). These data indicate that we can expect at most ≃5-7 field E/S0s per cluster image to I_{814}=23.0 whose colors mostly lie in the range $1< (V_{555}-I_{814}) <2$. The uncertainty in subtracting the field color distribution is sufficiently great that we prefer to use this number to give an indication of the number of discrepant points that it might be reasonable to consider eliminating in estimating the scatter on the colors.

In some samples, prior to obtaining the fits, we have eliminated a very small number (3-8%) of galaxies with highly anomalous ($V_{555}-I_{814}$) colors but in all cases the number so deleted lies within the estimates of field contamination. The bluest and faintest ($I_{814}> 22$) of these are generally quite compact and may in fact be field HII galaxies, rather than spheroidals. Obviously without spectroscopy of the $I_{814}> 22$ galaxies we cannot prove these anomalous objects are all field galaxies and thus it is certainly conceivable that there exist *some* faint spheroidal galaxies that are cluster members with anomalous colors. Although retaining these would increase the scatter in our faintest sample compared to the numbers we discuss below, their inclusion would produce an extended tail to the color distribution around a narrow core (as expected for field contaminants) and thus, as we seek a statistical result, the uncertain identity of these objects does not seriously affect our main conclusions.

3.2. UV-Optical Color-Magnitude Relations

Figure 4 shows the color-magnitude relations for each of the three clusters with different symbols for the important morphological types. The best fit to the total spheroidal population is drawn as well as that derived by BLE for their Coma E/S0 sample shifted to z=0.54 using the local giant elliptical SED adopted earlier (see below for further discussion).

In fitting the color-magnitude relation we have, with the assistance of Richard Bower, been able to use the same algorithm used by BLE in their analysis of the local Coma+Virgo samples. The fit parameters (A=intercept at I_{814}=21, B=slope) and the quality in terms of the rms residual for the various samples are given in Table 2. The intercept is evaluated at I_{814}= 21 to simplify comparisons for samples with different

slopes. Assuming a Gaussian distribution for the residuals around the fit we expect fractional errors in the quoted rms of 15%, 10% and 7% for sample sizes of 20, 50 and 100 galaxies respectively.

Looking at the various fits, it can be seen that the *slope* of the color-magnitude relation is relatively poorly constrained given the narrow apparent magnitude range available. It is consequently difficult to address the question of whether the three clusters are consistently drawn from a population with a single slope. The different richnesses of the three clusters is a further restriction in our analysis. Cl0016+16 contains more spheroidals than the other two clusters combined and thus dominates the statistics.

However, when we combine the samples for all three clusters, correcting only for differential redshift and reddening effects discussed in §3.1, we find that the overall slope for the deepest sample of 141 morphologically-classed spheroidals (E, E/S0 and S0) to I_{814}=23.0 is quite well-constrained (-0.070 ± 0.009). This value is not significantly changed by restricting the fit to the 93 galaxies to I_{814}=22.0. Ignoring the very small mismatch between $(V_{555}-I_{814})$ and rest-frame $(U-V)$ so far as the *slope* of the relation is concerned, the BLE fit to the Coma data to the same luminosity limit yields a color-magnitude slope of -0.082 ± 0.008, i.e. agreement to within $\sim 1\sigma$. We thus see little evidence evolution in the slope of the UV-optical color-magnitude relation for spheroidal galaxies out to $z = 0.54$, in line with expectations if metallicity differences, rather than age, is the prime cause of color differences in these distant cluster spheroids (Kodama & Arimoto 1996).

If we adopt the slope observed for the combined sample and fit the individual clusters to determine the variation in their intercepts we find the values listed in Table 2. These show a mean color of $(V_{555}-I_{814}) = 2.31 \pm 0.05$. Correcting for the scatter between the clusters expected from our calibration errors (± 0.04) this would indicate a dispersion between the mean colors in the three clusters of $\lesssim 0.03$, compared to the intrinsic scatter within each cluster, ± 0.07 (see below). We conclude that the differences between the mean colors of the spheroidal populations in these three clusters are certainly no larger than the internal scatter within the clusters.

The absolute comparison of the present-day color-magnitude relation in the context of the HST data requires a careful treatment of the mismatch between $(V_{555}-I_{814})$ and rest-frame $(U-V)$ and relies on our absolute photometric calibration of WFPC-2 discussed above. To make predictions, we have used the differential color matching techniques explained in detail by Aragón-Salamanca et al. (1993) and the results are shown on Figures 4. The predicted color-magnitude relations indicate an I_{814}= 21.0 galaxy in Cl0016+16 would have a color of $(V_{555}-I_{814}) = 2.68^{+0.02}_{-0.03}$ (where the error includes a contribution for the range in absolute luminosity in different cosmologies). The mean color observed for our clusters would thus imply $\Delta\,(V_{555}-I_{814}) = -0.37 \pm 0.06$ from z = 0–0.54. While early studies indicated little evolution in the colors of bright elliptical galaxies out to $z \sim 0.2$–0.5 (e.g. Wilkinson & Oke 1978; Kristian, Sandage & Westphal 1978), more recent work has reversed this conclusion. In particular our estimate is in reasonable agreement with the precision measurement of Aragón-Salamanca et al. (1993) for Cl0016+16 and Cl0054−27 (and the previous results of Ellis et al. (1985) and Couch et al. (1985) for these clusters), who find $\Delta\,(V-I) = -0.29 \pm 0.06$. The bluing trend observed for our data out to $z = 0.54$ is thus compatible with these estimates which have been interpreted as supporting a high redshift for the formation of the bulk of the stars in luminous cluster ellipticals (Aragón-Salamanca et al. 1993).

Any detailed interpretation of the rest-frame UV–optical color-magnitude relation at high redshift will unfortunately be affected by the uncertain contribution of hot stars in later stage of stellar evolution. Recent models (Yi 1996) suggest a greater contribution to the U-band light from such phases than assumed by BLE on the basis of Bruzual's (1983) models. Although it seems clear that post-main sequence produce the enhanced far-UV flux seen in local ellipticals (Demarque & Pinsonneault 1988; Dorman, Rood & O'Connell 1993), quantifying the effect depends on poorly-understood parameters, including the composition and mass loss on the red giant branch (Yi 1996). The important point to note here is that the observed *scatter*

around the C-M sequence, which is the principal measurement of interest here, should be an upper limit to that arising from main sequence stars.

3.3. UV-optical Scatter and Morphological Variations

We now turn to the prime motivation for the analysis, namely constraining the scatter about the best-fit relationship both internally within each cluster and for the combined sample after small corrections for differential reddening and redshift effects. As before, we have chosen to follow BLE's prescription as precisely as possible. Table 2 summarises the various rms values as a function of cluster, limiting magnitude and morphological class.

Only in Cl0016+16 is the sample large enough to attempt to measure the scatter for the Es and S0s classes separately. Regardless of sample definition, the tightness of the C-M relation is remarkably small (≤ 0.09 mag). There is also no evidence that the scatter for S0s is larger than that for those classed as Es. The intrinsic scatter in our sample can be obtained by subtracting the median photometric errors assessed earlier as a function of apparent magnitude in quadrature from the rms values measured to I_{814}=21.0, 22.0, 23.0 (Table 2). This indicates the *intrinsic scatter* is $\simeq$0.06$\pm$0.01 mag uniformly along the C-M sequence. Of the other two clusters, the scatter in the E+S0 sample for Cl0054−27 is comparable with that observed in Cl0016+16, while that in Cl0412−65 appears somewhat larger. A bootstrap estimate of the error in the Cl0412−65 measurement indicates an rms of 0.131 ± 0.027 mag, so the evidence for a larger scatter is marginal at best.

Having confirmed in the previous section that the scatter between the clusters is smaller than their internal dispersion, we next combine the data from the three clusters. The enlarged sample enables us to address possible morphological differences more carefully. As in Cl0016+16, the S0 population presents a similar C-M relation and scatter to that observed for the ellipticals. In an attempt to circumvent the problems with the misclassification of face-on S0's discussed above we also compare the scatter for those E and S0's with ellipticities above $\epsilon = 0.3$, where again we find that both samples show comparable scatter, ~ 0.07 mag. Although the fraction of morphologically-classified S0s is small overall (a point we will return to later), there is no convincing evidence for a broadening of their UV colours as might be expected if a substantial fraction had been transformed from spirals via environmental processes involving recent star formation.

In summary, the scatter of the rest-frame UV–optical C-M relation for morphologically-confirmed spheroidal galaxies at z=0.54 is small. To the same luminosity limit that BLE used in their analysis of the Virgo and Coma clusters, the combined intrinsic scatter for E+S0s across all three clusters is <0.07 mag, c.f. <0.035 locally (BLE), and the internal scatter in each cluster is comparable. There is no evidence of a systematic increase in the scatter when less luminous galaxies are included (to $M_V = -17.8 + 5\log h$) or between the E and S0 morphological samples, also in agreement with the analysis of local clusters (Sandage & Visvanathan 1978; BLE).

Finally, we have also looked for evolution of the colors *within* the spheroidal galaxies in these clusters. To do this we compare the color within our 0.7 arcsec radius aperture with that measured in an annulus between 0.7–1.5 arcsec radius ($\leq 11h^{-1}$ kpc). Taking the 51 elliptical galaxies lying on the C-M sequences in the clusters and for which we have good photometry (median I_{814}= 21.1) we obtain a median offset between the outer and inner regions of $\delta(V_{555} - I_{814}) = -0.082 \pm 0.037$, where the error is a bootstrap estimate of the variance of the median. For the average profile of our ellipticals, these annuli correspond to luminosity-weighted radii of 0.18 arcsec and 0.96 arcsec respectively. We therefore observe a color gradient

of $\delta(V_{555} - I_{814})/\delta(\log r) = -0.11 \pm 0.05$ per dex in these distant galaxies. The color gradients observed in local spheroidal galaxies are of the order of -0.20 ± 0.02 in $(U - R)$ and -0.09 ± 0.02 in $(B - R)$ (Peletier et al. 1990; Sandage & Visvanathan 1978). Converting these to $(U-V)$ gives $\delta(U-V)/\delta(\log r) = -0.16 \pm 0.03$, close to the value we obtain at $z = 0.54$. This indicates that there also has been little relative color evolution *within* these galaxies since $z \sim 0.5$, as expected if these galaxies were all formed at high redshift.

4. Star Formation History of Cluster Spheroidals

The tight scatter $\sigma(V_{555} - I_{814})$ we have found not only internally in our three clusters but also across the entire sample provides a significant new constraint on the history of star formation in rich cluster galaxies. Returning to the analysis of BLE and considering the close match between $(V_{555}-I_{814})$ and $(U-V)$ we can, to good precision, apply their original formula based on rest-frame $\delta(U-V)$:

$$\delta(U-V) = \frac{d(U-V)}{dt}\,\beta(t_H - t_F) \leq \sigma$$

where $d(U-V)/dt$ is well-understood and governed solely by main sequence lifetimes once the initial mass function is specified, t_H and t_F are respectively the cosmic age at the time of the observations and the look-back time from then to the epoch at which star formation in a single burst ended. β is a factor of order unity if the star formation history is uniformly distributed across the interval between the big bang and t_F. Values of β significantly less than unity imply smaller ages for a given σ but only at the expense of synchronising star formation across the sample within the characteristic collapse timescale, $t_H - t_F$ at a look-back time of t_F.

At low redshift, BLE grappled with separating β and t_F and concluded by offering a joint constraint (Figure 5 of BLE). Assuming σ <0.05 at $z \simeq$0 they placed the epoch of star formation as long ago as 13 Gyr for β=1, but concluded lower ages of 6–10 Gyr were allowed in the case where the spheroidals in Coma and Virgo had a more synchronised star formation history corresponding to β=0.1–0.3.

Whenever comparing ages derived from main sequence lifetimes with cosmological timescales the question of the value of the Hubble Constant necessarily arises. For the purposes of the discussion presented below we will therefore adopt $h = 0.5$ and note that using a larger value for h will tend to increase the redshift limits we derive, although a high enough value (e.g. $h = 1$) will lead to a conflict between the age of the Universe and the stellar lifetimes in standard cosmologies.

The most straightforward application of the BLE method is to assume the scatter arises from the random formation of spheroids within a 1 Gyr period which ended at t_F. The observed scatter of <0.07 mag gives a minimum age of $t_F \simeq$5 Gyr *when viewed from a redshift of 0.54* irrespective of other assumptions. A more elaborate treatment invoking β=1 but based on a 1 Gyr burst in a cosmology with t_H=15 Gyr as assumed by BLE ($h = 0.5$), gives a similar minimum age of 6 Gyr (Figure 6). As discussed in detail by BLE, as the rate of change of $(U-V)$ with time is governed primarily by the rate at which the main-sequence turnoff evolves redward, such ages depend only weakly on the slope of the IMF and upon metallicity (Iben & Renzini 1984).

At high redshift, the "β problem" is less important for two reasons. Firstly, we have witnessed that across *three* clusters there is no convincing evidence that the cluster-cluster scatter is significantly larger than that observed internally. Yet, it would certainly appear that the three clusters are rather different in their evolutionary histories, e.g. Cl0016+16 is much more massive, richer and X-ray luminous than

Cl0412−65. It would be difficult to argue that the rate of star formation in the respective cluster galaxies could evolve at the same rate unless *either* spheroidal galaxies evolve as closed boxes with no interference from their local environment *or* the epoch of star formation was quite a long time earlier.

Secondly, if the primary goal is to establish whether or not spheroidal galaxies formed in a single burst at high redshift, the compression of look-back time at high redshift means that β uncertainties are far less troublesome when interpreting the UV–optical scatter at z=0.54 as compared to that viewed by BLE at z=0. For example, in a cosmology with $h = 0.7$ $\Omega_o = 0.05$, an age of >6 Gyr at z=0.54 (corresponding to β=1) implies major star formation must have occurred before $z_F \simeq 3$ when the age of the Universe was only ≃3 Gyr old. For $\Omega_o = 1$, elliptical galaxies join the age dilemma associated with globular clusters unless H_o is significantly lower. The important point here is not the precise era of formation but simply that *any* β larger than 0.3 implies cluster spheroidals formed most of their stars well before a redshift of 3. Indeed, this era can only be brought *below* z ≃3 if the formation is unreasonably synchronised (β ≃0.1) or by invoking a world model with a dominant cosmological constant (Ω_Λ ≃0.8).

It is tempting to consider combining the BLE and present data into a statement about the considerable age of *all* cluster spheroidals. Certainly, BLE's estimates on the residual star formation allowed for Virgo and Coma were *upper limits* entirely consistent with the new constraints found here. However, as Kauffmann (1996) has argued, by selecting the richest clusters at a given redshift for study, we are unlikely to be observing the precursors of present-day clusters. Likewise, Franx & van Dokkum (1996) have warned of the selection effects that might operate if ellipticals are identified in ways that guarantee they are at least 2–3 Gyr old at any redshift. It is certainly possible that the luminous ellipticals in Coma and Virgo are somewhat younger than those studied here and we cannot exclude the possibility that more luminous ellipticals will form in, say, Cl0016+16 subsequent to the time of our observation. However, the latter does seem unlikely given the elliptical fraction is already very much higher than in many local clusters. The most robust statement we can make from the present study is that the stars that form the dominant proportion of the red light in three $z \sim 0.54$ clusters formed before z ≃3.

We have also shown that the differences in the mean colors of the spheroidal galaxies in the three clusters are smaller than the intrinsic dispersion within any one cluster ($\lesssim 0.03$ versus $\lesssim 0.07$). The relatively wide range in cluster masses for our sample would then indicate that spheroidal galaxies in rich clusters were *all* formed within a relatively short period of time. However, there is expected to be some scatter between the collapse times of the structures in which the ellipticals formed, at a fixed mass, depending upon the final mass of the structure in which they are forming. The small cluster-to-cluster scatter would indicate that the environmental variation in the mean collapse times is smaller than the intrinsic dispersion in collapse times for halos, which will all form similar luminosity galaxies.

Two important questions emerge from the above discussion. Firstly, to what extent can we generalise the conclusion concerning the bulk of the starlight in these three clusters to the majority of rich clusters? It certainly seems reasonable to consider that our conclusions might apply to those galaxies that form the 'red envelope' in the larger sample of 10 clusters tracked by Aragón-Salamanca et al. (1993) to $z \sim 0.9$. Although those authors did not have access to morphological data, the scatter in the $(V - K)$ color of the red envelope from cluster to cluster at a given redshift is similarly small and the photometric color evolution, when interpreted in the framework of Bruzual's (1983) models, indicates a high redshift of star formation. To generalise our result however, we would need to address the selection criteria for the clusters themselves, as well as the volume density of red starlight so located compared to the present-day value. As none of the clusters in the present dataset, or in Aragón-Salamanca et al's study, were found using well-defined search criteria, it is not possible to make further progress.

The second question is to what extent we can quantify the proportion of *present-day* spheroidals which have the properties we have assigned to the sample seen at $z = 0.54$? This is crucial to understand when

one considers recent attempts to track the fundamental plane to moderate redshifts (van Dokkum & Franx 1996; Barger et al. 1996b). Although related to the first question in the sense that any evolution of the morphological content of clusters with redshift cannot be detached from understanding how the clusters themselves were selected, we immediately note from Table 2 that the E:S0 ratio in our high redshift clusters is far higher than that observed in present-day clusters like Coma and Virgo. Thus although we find no evidence that those few (predominantly luminous) S0s formed their stars any later than the more dominant ellipticals, clearly the mixture has evolved since $z = 0.54$ in the sense that points to continued production of S0s. This point is discussed more fully in the context of the evolution of the morphology-density relation in the sample discussed by Dressler et al. (1996).

If our results are typical of high redshift clusters, as seems reasonable given earlier work, what can we expect to see during the primeval star-forming phase? Traditionally, such systems were thought to be spectacularly luminous placing them well within the range of faint optical redshift surveys (Tinsley 1977). The absence of a bimodal redshift distribution at faint limits (Lilly et al. 1995; Cowie et al. 1996) makes this picture difficult to support unless the redshift of formation is very high. A more likely explanation is the hierarchical merging picture elucidated by Baugh et al. (1996) and Kauffmann (1996). In this picture, a rapid era of star formation at $z > 3$–4 involves sub-units of lower intrinsic luminosity which subsequently merge and assemble the galaxies seen at $z = 0.54$. Kauffmann claims the merging history can be made consistent with our measured $(V_{555} - I_{814})$ scatter if it occurs primarily before a redshift $z \simeq 2$ (c.f. her Figure 3), at such an early epoch it would appear to be somewhat semantic whether a halo collapse is described as a merger or not.

In recent months, the first glimpse of a possibly normal galaxy population at redshifts $z \gtrsim 3$ has emerged via Lyman limit selected samples in the Hubble Deep Field (van den Bergh et al. 1996; Clements & Couch 1996; Giavalisco et al. 1996; Steidel et al. 1996b) and in other faint fields (Steidel et al. 1996a). The redshifts of many of these objects have now been confirmed spectroscopically. Morphologically they are found to be small objects; many are multiple and all are blue and undergoing moderate star-formation.

It is tempting to interpret these high redshift systems as ancestors of the spheroidal population. Crucial to this interpretation however, is an estimate of the mass associated with the $z \simeq 3$ objects as well as an estimate of their volume density in the context of the present-day population. At this stage neither connection can be convincingly established. However, we would note that the principle conclusion of our study is that the main star formation era for cluster spheroidals occurred before $z \simeq 3$, i.e. possibly in the regime of the Lyman-limit samples and that these are most likely the oldest galaxies of all. The connection with the Lyman limit samples is therefore certainly suggestive when one considers the *rarity* of the population observed beyond $z \simeq 3$.

5. Conclusions

We have analysed the photometric properties of a large sample of morphologically-selected spheroidal galaxies in three clusters of mean redshift $z = 0.54$ and shown how it is possible to derive constraints on the nature of the Universe beyond $z \simeq 3$ from precision studies at more modest redshifts. We can summarise our main conclusions as follows:

1. We demonstrate, through simulations and other tests that we can easily differentiate between spheroidal galaxies and disk systems to at least I_{814}=22.0 in WFPC-2 images of a few orbits' duration.

2. We find that the rest-frame UV-optical color-luminosity relation has approximately the same slope at z=0.54 as it does locally with only a modest bluing, $\Delta \simeq -0.3$ mag, consistent with evolution inferred from earlier ground-based studies.

3. The scatter in the rest-frame UV-optical color-luminosity relation at $z = 0.54$ is found to be ≤ 0.1 mag rms to I_{814}=23.0 with no evidence of any luminosity-dependent scatter down to absolute magnitudes of $M_V = -17.8 + 5 \log h$. In the combined samples, there is no evidence that the S0 population has a greater scatter than the more numerous ellipticals, a similar result to that found locally (Sandage & Visvanathan 1978; BLE).

4. Significantly, the external scatter in the color-luminosity relation between the three clusters is smaller than the internal scatter within each cluster. Given the relatively large range in cluster properties within our sample, this would imply that the formation epoch for the stellar populations in the cluster spheroids is fairly insensitive to the cluster properties.

5. In the context of the earlier work of Bower, Lucey & Ellis (1992), we can understand the tight scatter in rest-frame UV-optical colors only if the bulk of the star-formation in the dominant spheroidal cluster galaxies occurred about 5–6 Gyr earlier than the era at which they are observed. In conventional cosmologies without a dominant Λ term, this implies a redshift $z_F > 3$ for $h = 0.5$. This high redshift is consistent with the modest bluing of their stellar populations we observe between $z = 0$ and $z = 0.54$.

6. Although our result does not preclude the continued formation of spheroidal galaxies in clusters or in the field at lower redshift, within the context of hierarchical models, an important implication of our result should be the detection of a population of star-forming sub-units with $z > 3$ as recently verified with Keck spectroscopy.

Acknowledgements

We wish to thank Ray Lucas at STScI for his invaluable assistance which enabled the efficient gathering of these observations. We also thank Barry Madore for generously providing the high quality ground-based images of our clusters necessary for their calibration. We thank the referee, Dr. Allan Sandage, for his clear and precise comments which have helped clarify the structure of this paper. We acknowledge important contributions from Bob Abraham, Amy Barger, Bianca Poggianti and, especially, Richard Bower whose methods we have closely followed in this study. Finally we thank Alvio Renzini and Michael Rich for their consistent encouragement.

REFERENCES

Abraham, R.G., Tanvir, N.R., Santiago, B.X., Ellis, R.S., Glazebrook, K. & van den Bergh, S., 1996a, MNRAS 279, L47.

Abraham, R.G., van den Bergh, S., Glazebrook, K., Ellis, R.S., Santiago, B.X., Surma, P. & Griffiths, R.E., 1996b, ApJ, in press (November issue).

Aragón-Salamanca, A., Ellis, R.S. & Sharples, R.M., 1991, MNRAS, 248, 128.

Aragón-Salamanca, A., Ellis, R.S., Couch, W.J. & Carter, D., 1993, MNRAS, 262, 764.

Baade, W., 1958, in *Stellar Populations*, ed. O'Connell, D.J.K., Vatican Observatory, p 3.

Barger, A., Aragón-Salamanca, A., Ellis, R.S., Couch, W.J., Smail, I. & Sharples, R.M., 1996a, MNRAS, 279, 1.

Barger, A., Aragón-Salamanca, A., Smail, I., Ellis, R.S., Couch, W.J., Dressler, A., Oemler, A., Butcher, H. & Sharples, R.M., 1996b, in preparation.

Baugh, C., Cole, S. & Frenk, C.S., 1996, MNRAS, submitted.

Bertin E. & Arnouts, S., 1996, A&AS, 117, 393.

Bower, R.G., Lucey, J.R. & Ellis, R.S., 1992, MNRAS 254, 601 (BLE).

Bower, R.G., Böhringer, H., Briel, U.G., Ellis, R.S., Castander, F.J. & Couch, W.J., 1994, MNRAS, 268, 345.

Bower, R.G., Castander, F.J., Couch, W.J., Ellis, R.S. & Böhringer, H., 1996, MNRAS, submitted.

Bruzual, G., 1983, ApJ, 273, 105.

Carlberg, R. et al., 1996, in press.

Clements, D. & Couch, W.J., 1996, MNRAS 280, L43.

Colless, M., Ellis, R.S., Taylor, K. & Hook, R.N., 1990, MNRAS, 244, 408.

Couch, W.J., Ellis, R.S., Godwin, J. & Carter, D., 1984, MNRAS, 205, 1287.

Couch, W.J., Shanks, T. & Pence, W.D., 1985, MNRAS, 213, 215.

Couch, W.J, Ellis, R.S., Maclaren, I. & Malin, D.F., 1991, MNRAS, 249, 606.

Cowie, L.L., Songaila, A., Hu, E.M., Cohen, J.G., 1996, AJ, in press.

de Vaucouleurs, G., de Vaucouleurs, A., Corwin, H.G., Buta, R., Patrel, G. & Fougué, P., 1991, *Third Reference Catalog of Bright Galaxies*, Springer New York.

Demarque, P. & Pinsonneault, M.H. 1988 in *Profess and Opportunities in Southern Hemisphere Optical Astronomy*, eds. Blanco, V.M. & Phillipps, M.M., ASP, p 371.

Dorman, B., Rood, R.T. & O'Connell, R., 1993, ApJ, 419, 596.

Dressler, A., 1984, ApJ 281, 512.

Dressler, A. & Gunn, J.E., 1992, ApJS, 75, 1.

Dressler, A., Oemler, A. Jr, Smail, I., Couch, W.J., Ellis, R.S., Barger, A., Butcher, H., Poggianti, B.M. & Sharples, R.M., 1996, submitted.

Dressler, A., et al. 1997, in preparation.

Driver, S.P., Windhorst, R.A., Ostrander, E.J., Keel, W.C., Griffiths, R.E. & Ratnatunga, K.U., 1995, ApJ, 449, L23.

Ellis, R.S., Couch, W.J., MacLaren, I. & Koo, D.C., 1985, MNRAS, 217, 239.

Franx, M. & van Dokkum, P.G. 1996, *New Light on Galaxy Evolution*, eds. Bender, R. & Davies, R.L., in press.

Frei, Z., Guhathakurta, P., Gunn, J.E. & Tyson, A.J., 1996, AJ, 111, 174.

Glazebrook, K., Ellis, R.S., Santiago, B.X. & Griffiths, R.E., 1995, MNRAS, 275, L19.

Giavalisco, M., Steidel, C.C. & Macchetto, F.D., 1996, ApJ Lett, 470, 189.

Holtzman, J.A., Burrows, C.J., Casertano, S., Hester, J.J., Trauger, J.T., Watson, A.N. & Worthey, G., 1995, PASP, 107, 1065.

Iben Jr, I. & Renzini, A., 1984, Phys Reports, 105, 329.

Kauffmann, G., 1996, preprint. (astro-ph/9502096)

Kodama, T. & Arimoto, N., 1996, A&A, in press. (astro-ph/9609160)

Koo, D., ApJ Lett, 1981, 251, L75.

Kristian, J., Sandage, A. & Westphal, J.A., 1978, ApJ, 221, 383.

Lilly, S.J., LeFévre, O., Crampton, D., Hammer, F. & Tresse, L., 1995, ApJ, 455, 50

MacLaren, I., Ellis, R.S. & Couch, W.J., 1988, MNRAS 230, 249.

Mihos, C., 1995, ApJ, 438, L75.

O'Connell, R.W., 1980, ApJ, 236, 340.

Oemler, A., 1991, in *Clusters & Superclusters of Galaxies*, ed. Fabian, A.C., Kluwer, p29.

Quinn, P., 1984, ApJ, 279, 596.

Rose, J.A., Bower, R.G., Caldwell, N., Ellis, R.S., Sharples, R.M. & Teague, P., 1994, AJ, 108, 2054.

Sandage, A. & Visvanathan, N., 1978, ApJ, 223, 707.

Smail, I., 1993, Ph.D. thesis, University of Durham

Smail, I., Ellis, R.S. & Fitchett, M.J., 1994, MNRAS, 270, 245.

Smail, I., Ellis, R.S., Dressler, A., Couch, W.J., Oemler, A., Sharples, R.M. & Butcher, H., 1996a, ApJ, in press.

Smail, I., Dressler, A., Couch, W.J., Ellis, R.S., Oemler, A., Butcher, H., & Sharples, R.M., 1996b, ApJS, submitted. (S96)

Steidel, C.C., Giavalisco, M., Pettini, M., Dickinson, M. & Adelberger, K.L., 1996a, ApJ Lett, in press.

Steidel, C.C., Giavalisco, M., Dickinson, M. & Adelberger, K.L., 1996b, AJ, 112, 352.

Tinsley, B.M. & Gunn, J.E., 1976, ApJ, 302, 52.

Tinsley, B.M., 1977, ApJ, 211, 621.

Toomre, A., 1978, in *Evolution of Galaxies & Stellar Populations*, eds. Tinsley, B.M. & Larson, R., Yale Univ. Press., p401.

Worthey, G., 1995, ApJ, 95, 107.

van den Bergh, S., Abraham, R.G., Ellis, R.S., Tanvir, N.R., Santiago, B.X. & Glazebrook, K., 1996, AJ, 112, 359.

van Dokkum, P.G. & Franx, M., 1996, MNRAS, 281, 985.

Wilkinson, A., & Oke, J.B., 1978, ApJ, 220, 376.

Yi, S., 1996, Ph.D. thesis, Yale University

Figure 1: WFPC-2 images in the F814W band for three high redshift clusters, (a) Cl0016+16 ($z = 0.54$), (b) Cl0054−27 ($z = 0.56$) and (c) Cl0412−65 ($z = 0.51$). Objects marked represent morphologically-selected early-type galaxies (E, E/S0 and S0) to I_{814}=23.0.

This preprint was prepared with the AAS LaTeX macros v3.0.

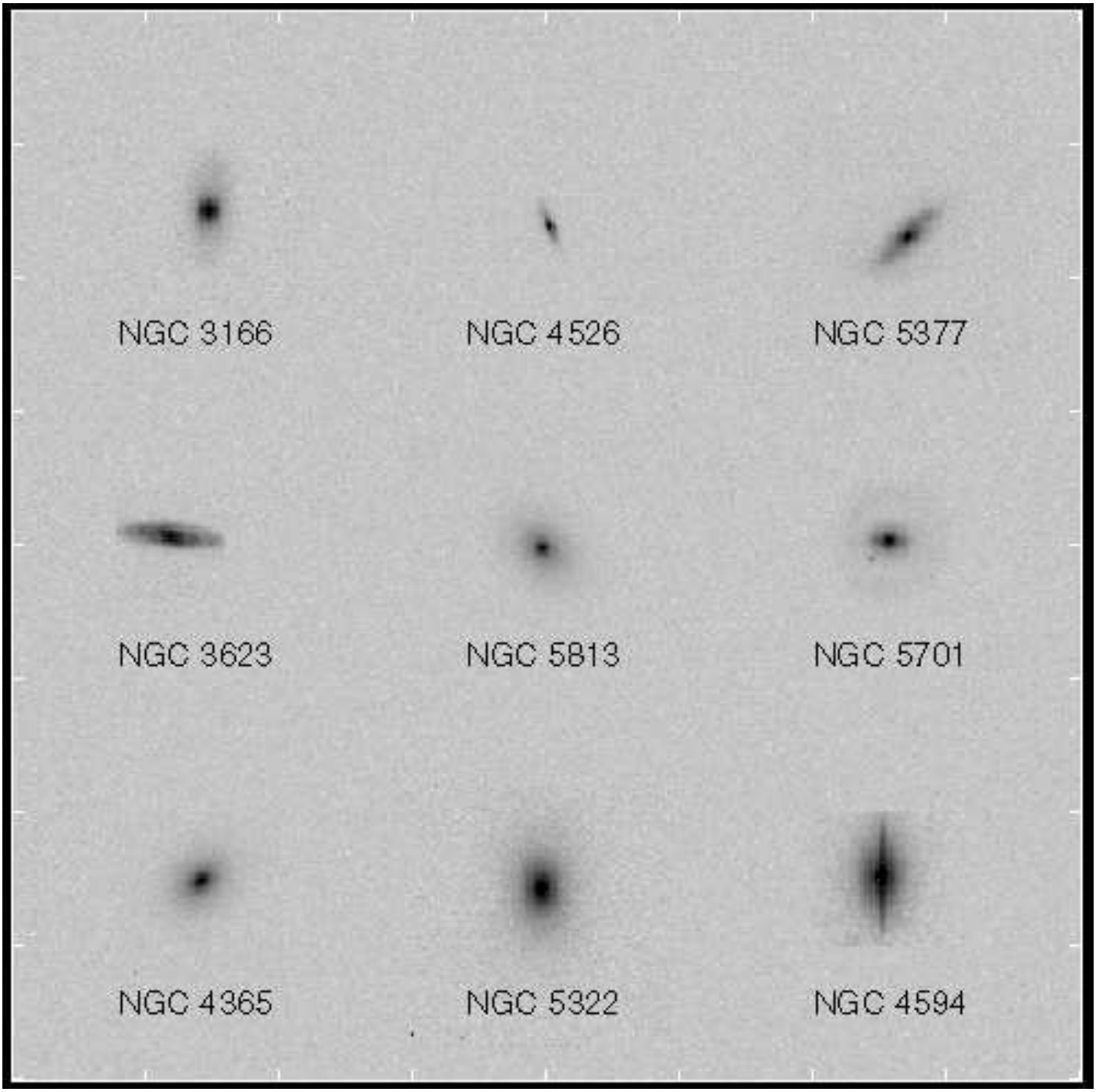

Figure 2: The simulated appearance of representative local E, S0 and early type spirals as they would appear when placed at a redshift $z = 0.5$ and observed with WFPC-2 using parameters equivalent to the "MORPHS" survey. NGC 5813, 4365 and 5322 are Es, NGC 4526 is a S0, NGC 5377 and 3623 are Sa's and NGC 4594, 5701 and 3166 are S0/a. Classifications for these galaxies come from the RC3 (de Vaucouleurs et al. 1991). The simulations were kindly performed by Roberto Abraham and take into account pixel-by-pixel k-correction and surface brightness effects with WFPC-2 specific parameters as discussed by Abraham et al. (1996b).

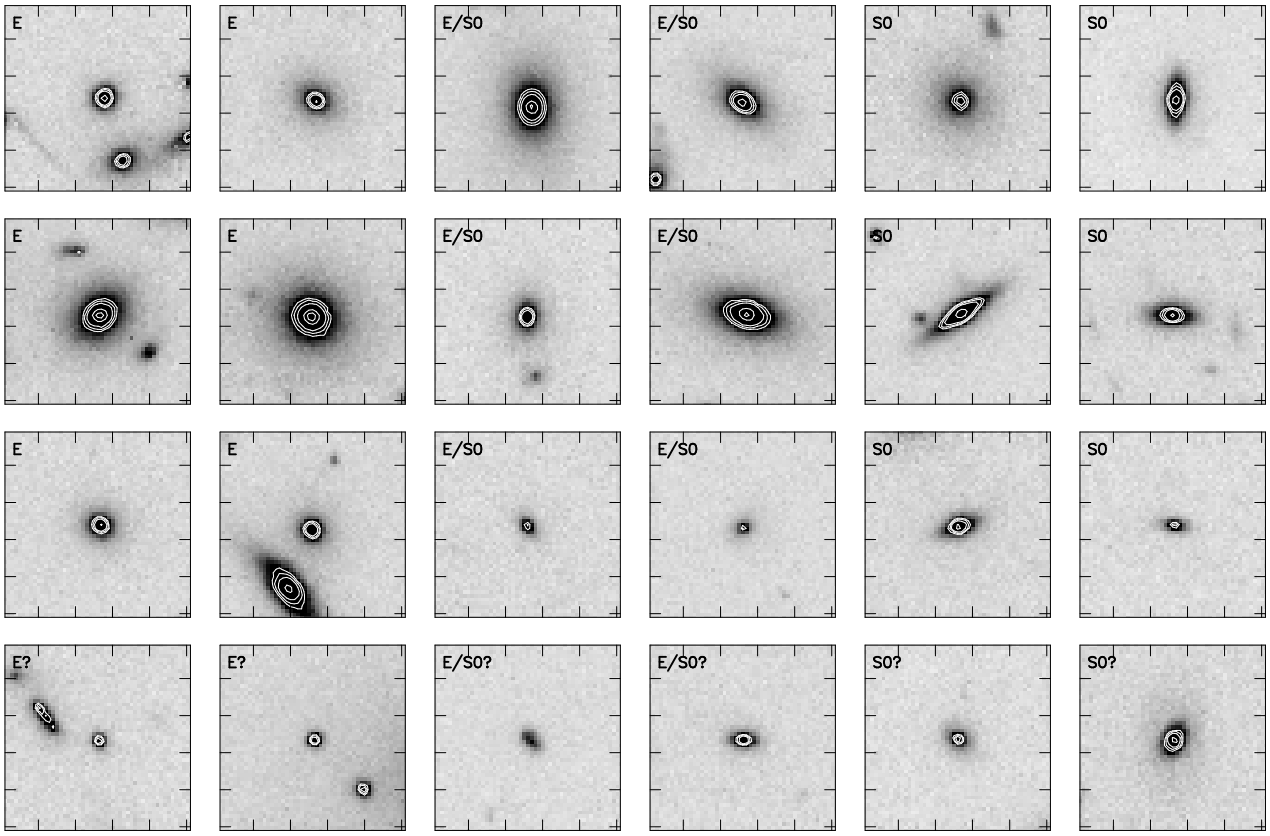

Figure 3: A mosaic of F814W images and morphological classifications for representative spheroidal galaxies in our three clusters. The top two rows indicate galaxies in the bright sample $I_{814} < 21.0$ with the sub-class indicated according to a scheme E : E/S0 : S0 (see text). The third row indicates objects classed as elliptical to the fainter limit $21.0 < I_{814} < 23.0$. The bottom row shows spheroidal galaxies for which there is some disagreement amongst the classifiers (see text for details). The individual images are 10×10 arcsec, roughly equivalent to $40\ \mathrm{h}^{-1} \times 40\ \mathrm{h}^{-1}$ kpc at the distance of our clusters.

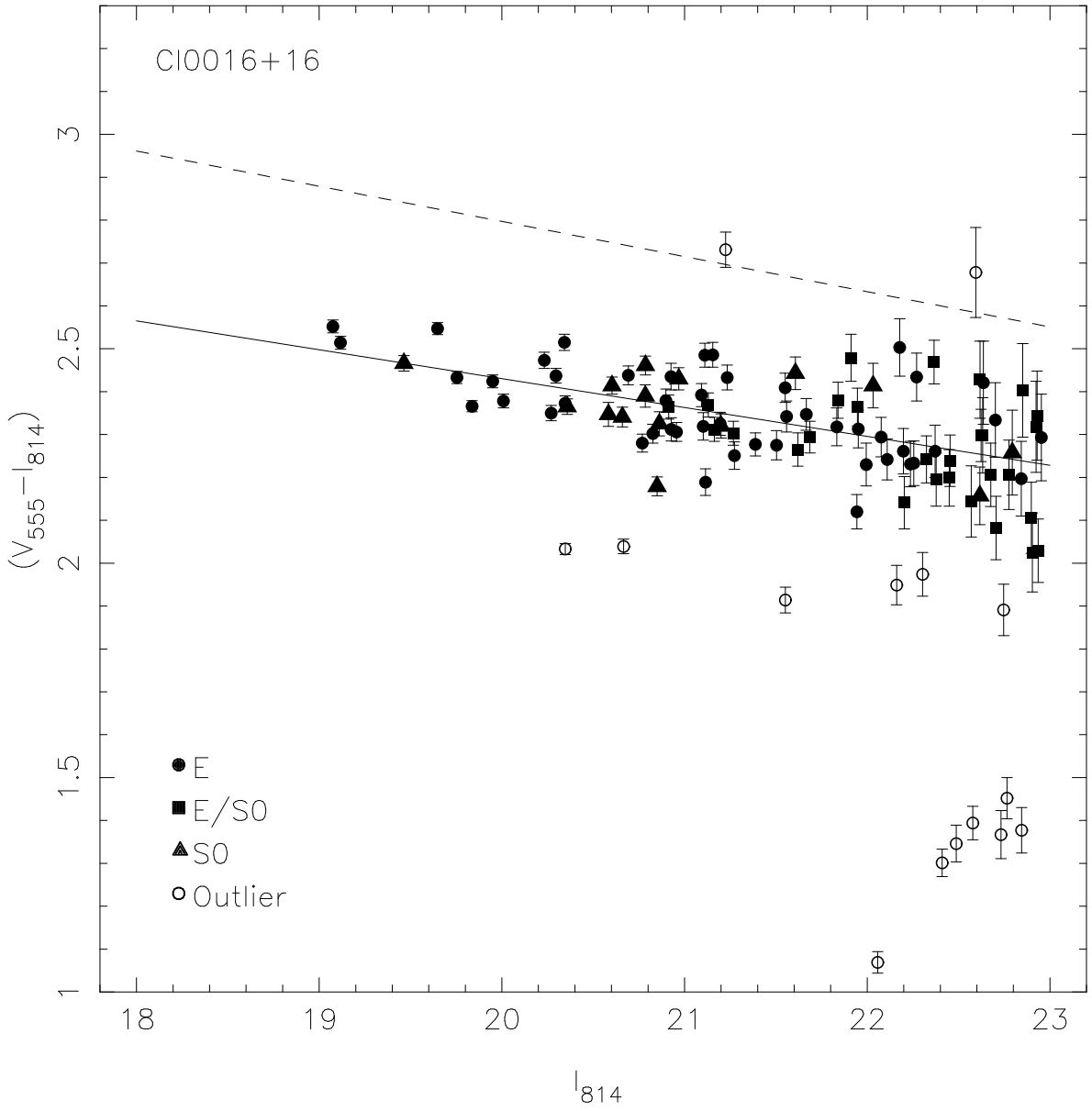

Figure 4 The $(V_{555}-I_{814})$–I_{814} color-magnitude diagrams for the three clusters after transforming them to the Cl0016+16 observed frame, (a) Cl0016+16, (b) Cl0054−27 and (c) Cl0412−65. Es are indicated by filled circles, S0's by triangles and E/S0s by squares. Those spheroidals and compact objects known to be field galaxies or discounted from the analysis are indicated by open circles. We overplot the best linear fits (Table 2) to the color-magnitude relation of the spheroids (E, E/S0 and S0's) and the dashed line represents the local BLE relationship as it would appear at z=0.54 in the absence of any color evolution.

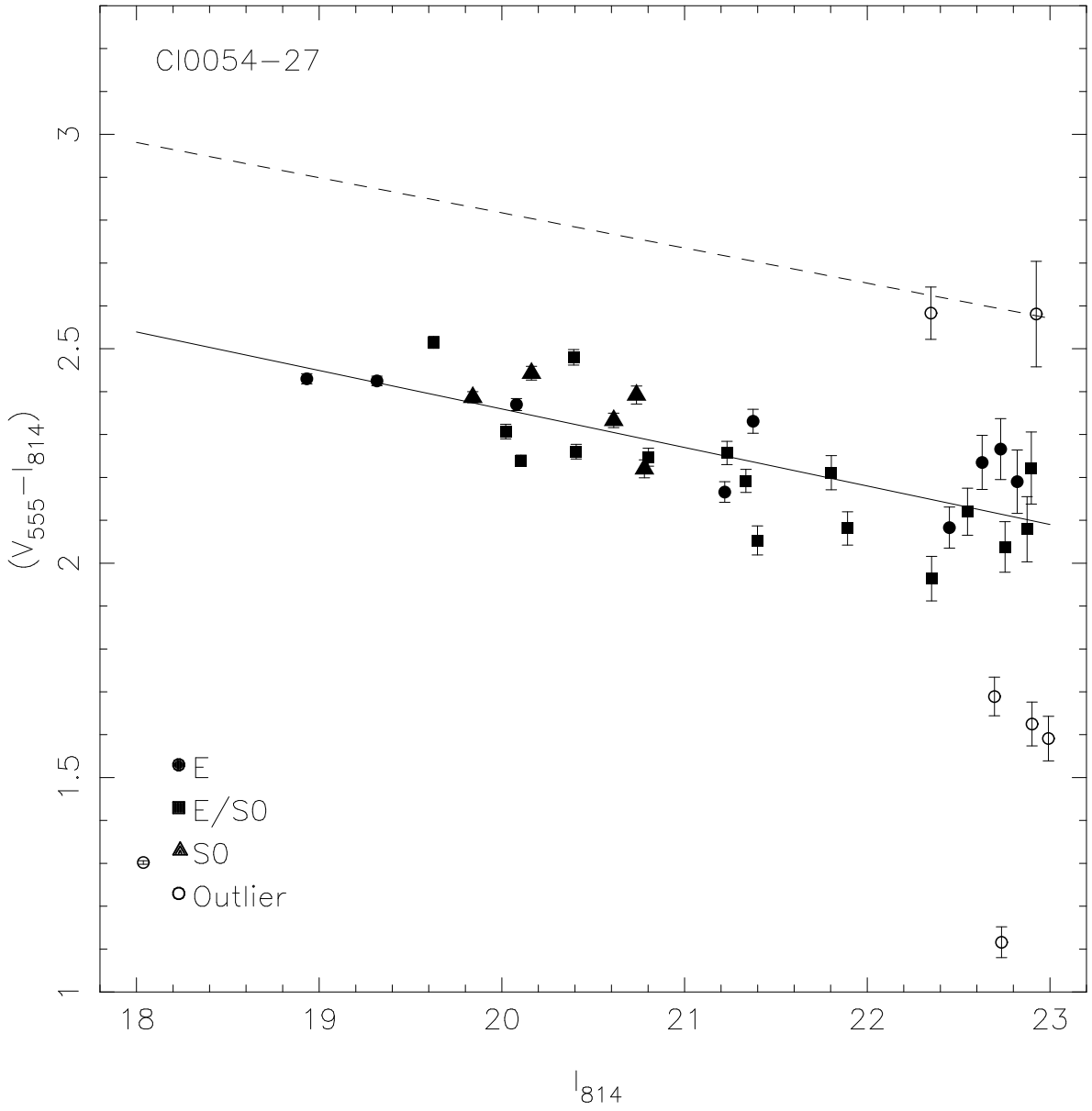
Cl0054−27
E
E/S0
S0
Outlier
$(V_{555}-I_{814})$
I_{814}
1
1.5
2
2.5
3
18
19
20
21
22
23

Figure 4b

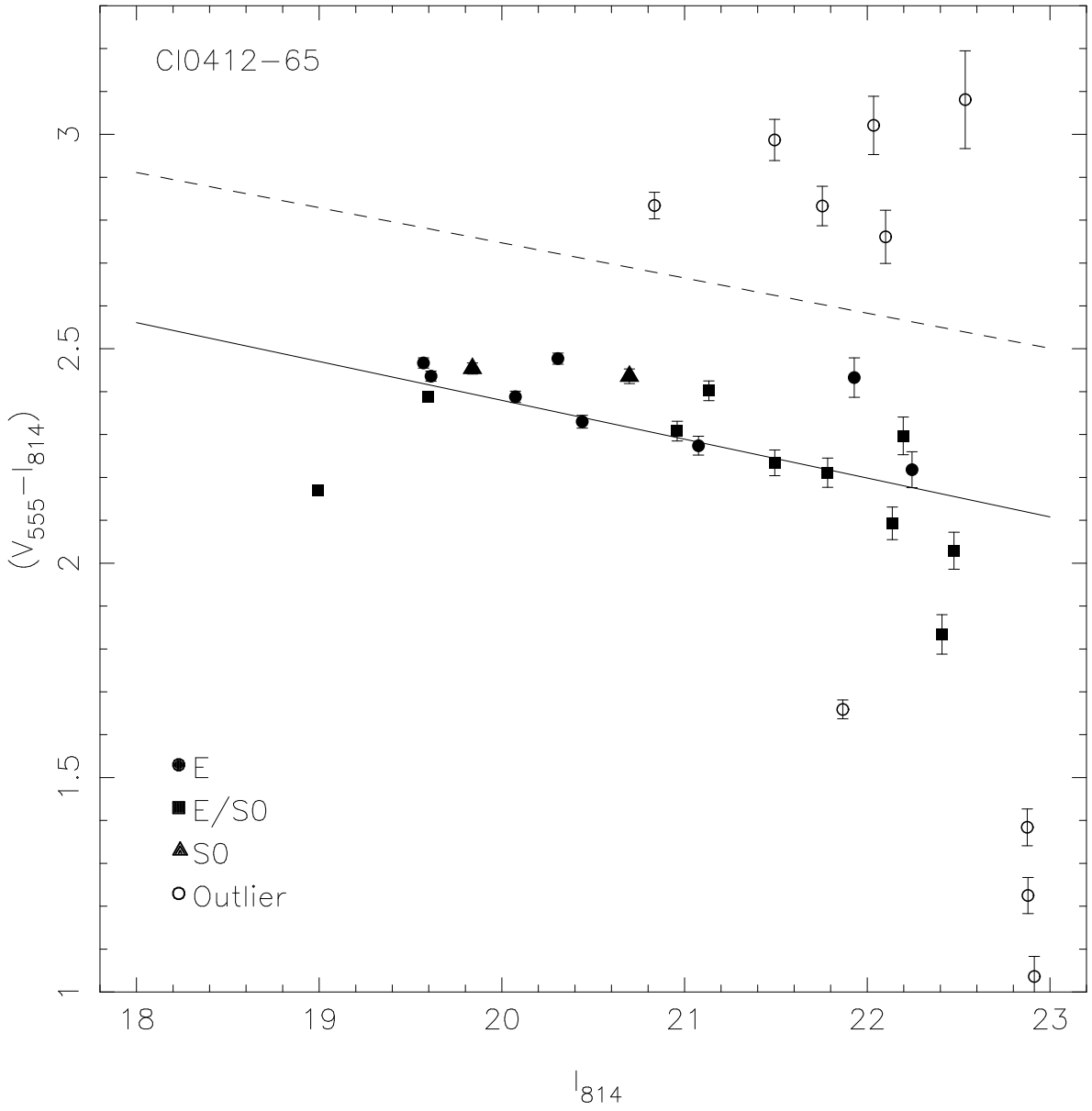
Cl0412−65
E
E/S0
S0
Outlier
$(V_{555}-I_{814})$
I_{814}
1
1.5
2
2.5
3
18
19
20
21
22
23

Figure 4c

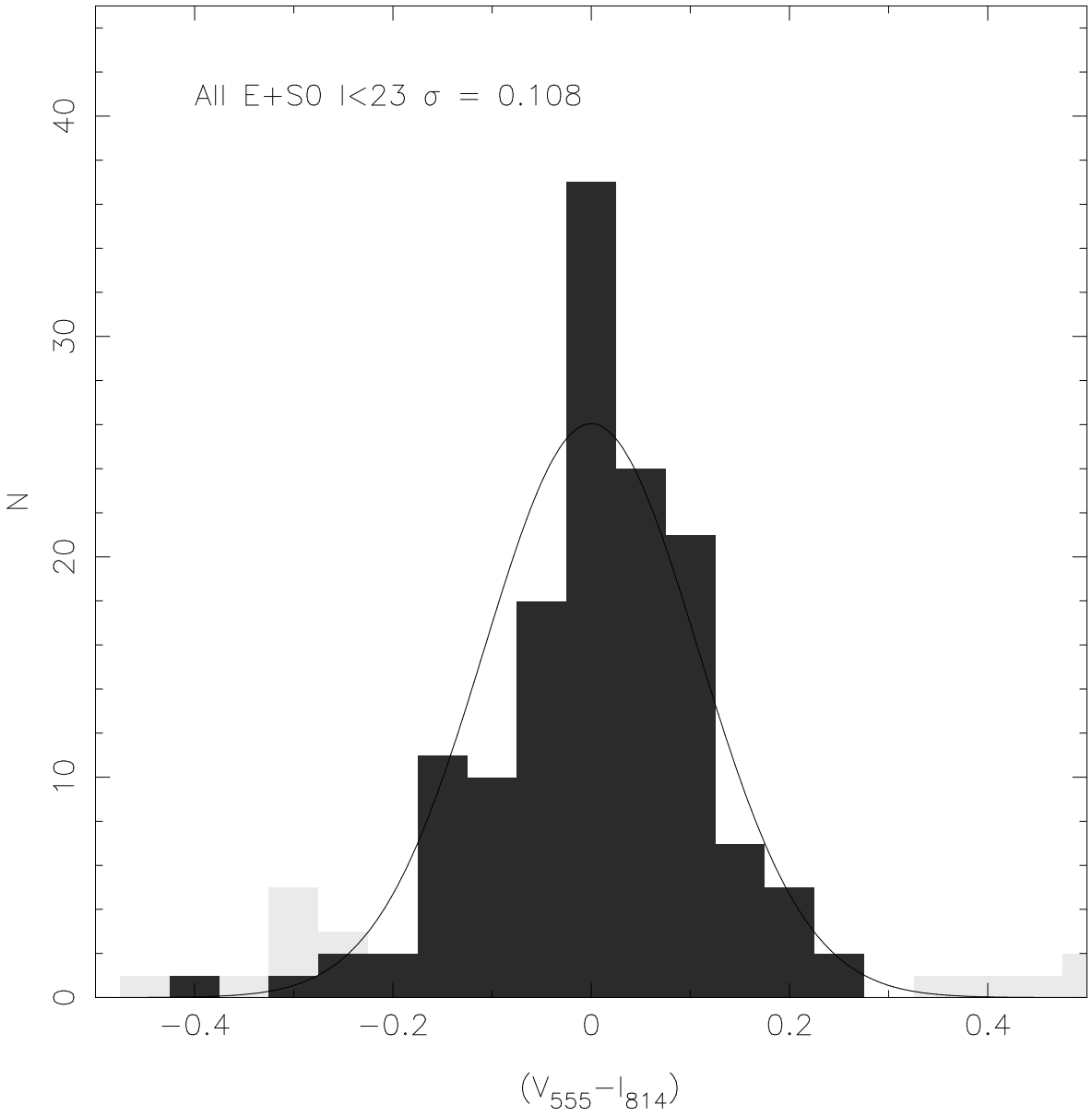

Figure 5: (a) The distribution of $(V_{555}-I_{814})$ color residuals for spheroids (E, E/S0 and S0's) in the combined cluster sample to I_{814}=23.0 after removing the mean color magnitude slope (see text for details). Light shaded objects refer to those eliminated in the fits. (b) The similar distribution for elliptical galaxies (E-only) from all three clusters to a limit of I_{814}=22.0. This has been corrected for the mean color magnitude slope (see text for details). (c) The distribution of $(V_{555}-I_{814})$ color residuals for all the S0 galaxies brighter than I_{814}=22.0 in the combined cluster sample, after correcting for the mean color magnitude slope.

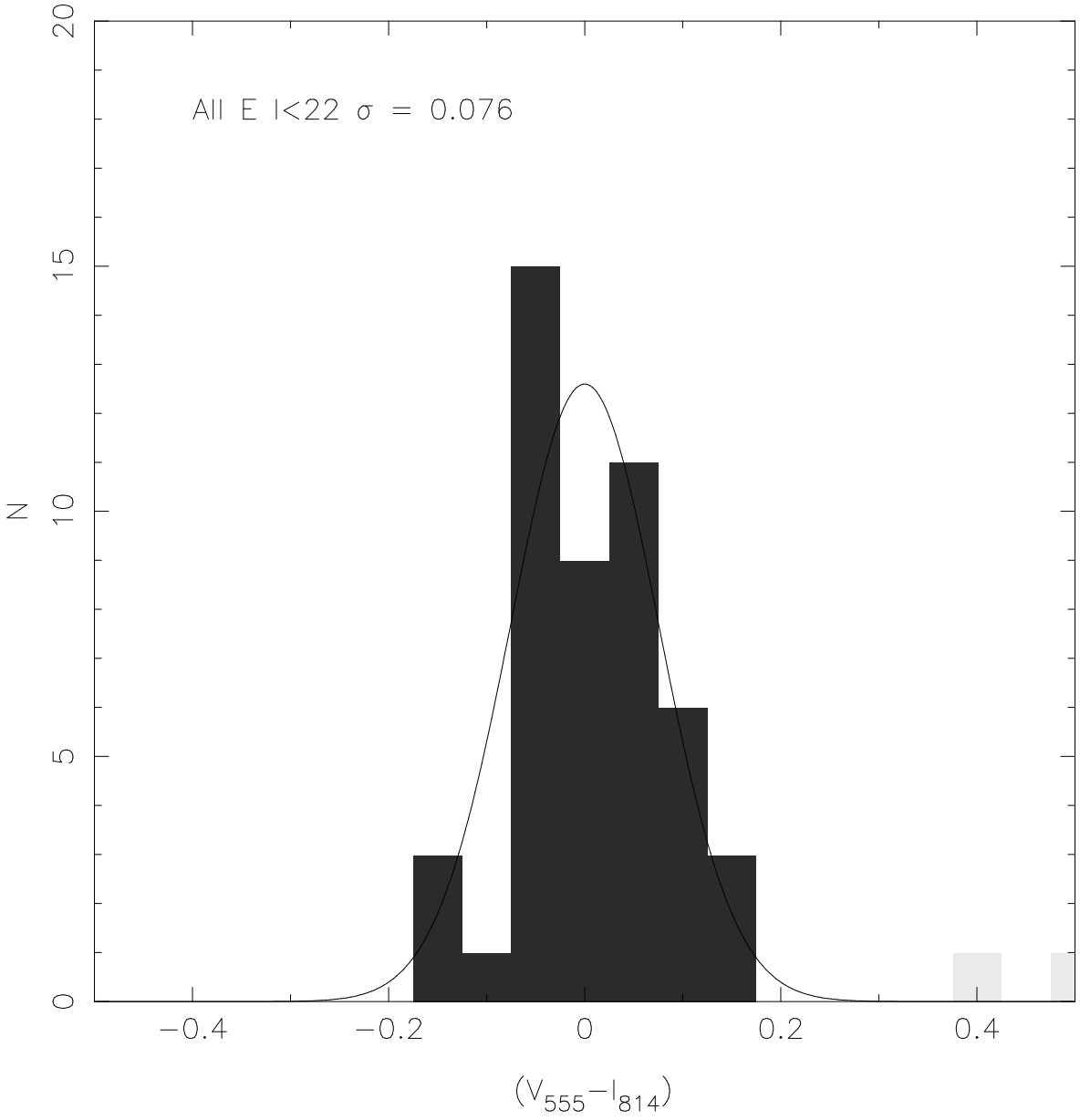

Figure 5b

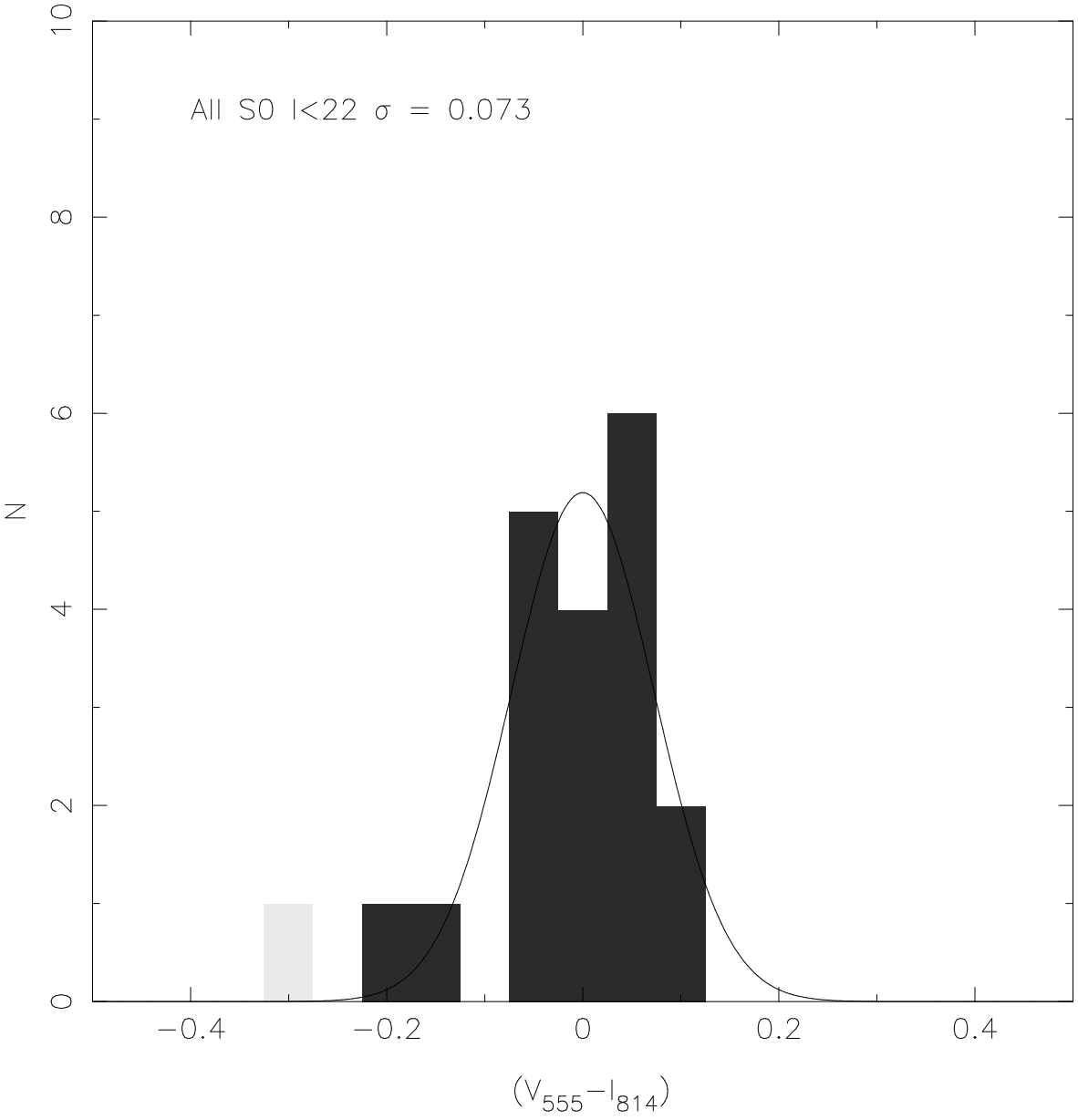

Figure 5c

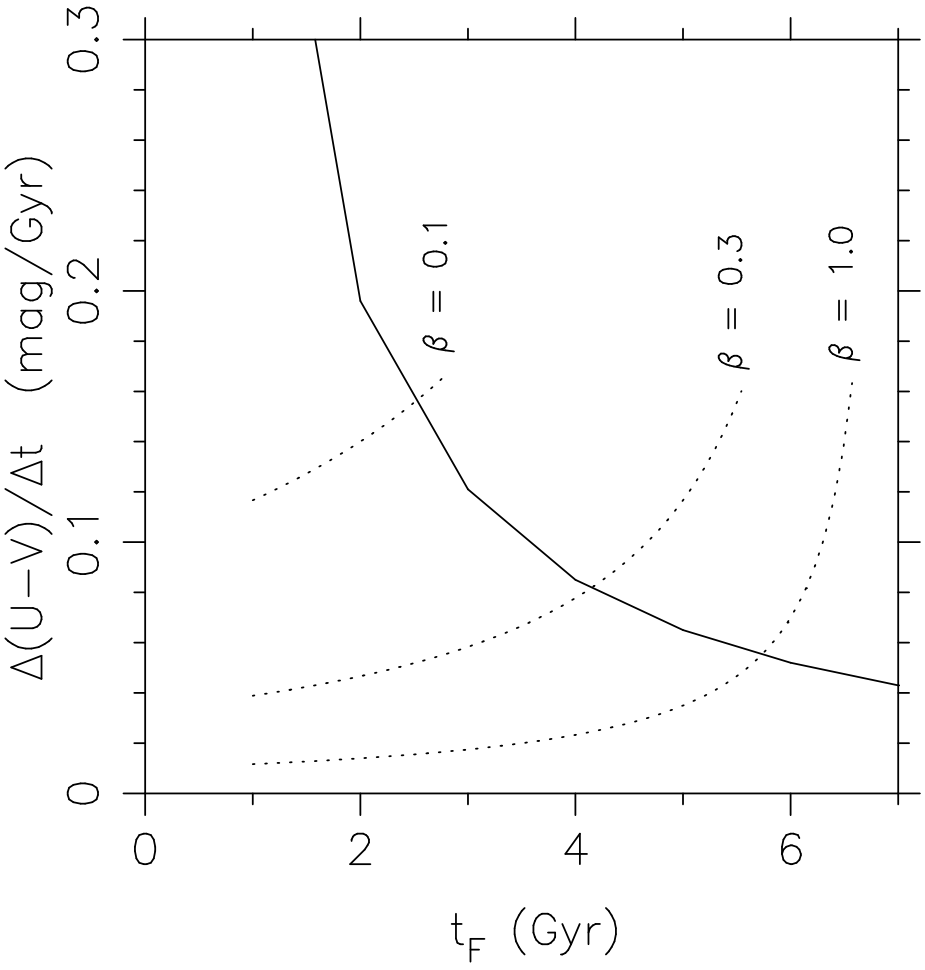

Figure 6: The solid line shows the rate of change of galaxy color as a function of time since the formation epoch t_F after a single burst of star formation of duration 1 Gyr. Assuming the observations refer to a cosmic age t_H associated with $z = 0.54$, the observed scatter in colors, σ, places an upper limit on the allowed rate of color evolution according to the criterion: $\delta(U-V)/\delta t < \sigma/\beta(t_H - t_F)$, where β is a factor that allows any synchronisation in the formation history (see text). The dotted lines indicate minimum ages *at the time of observation* for various values of β.

Table 1
Cluster Sample

Cluster	α J2000	δ J2000	z	L_X 10^{44} ergs sec^{-1}	T_{exp} (ks) F555W	F814W
Cl0016+16	$00^h18^m33\overset{s}{.}64$	$+16°25'46\overset{''}{.}1$	0.546	23.5	12.6	14.7
Cl0054−27	$00^h56^m54\overset{s}{.}59$	$-27°40'31\overset{''}{.}3$	0.563	1.0	12.6	16.8
Cl0412−65	$04^h12^m51\overset{s}{.}65$	$-65°50'17\overset{''}{.}5$	0.510	0.3	12.6	14.7

Table 2
Color-magnitude Results

Cluster	**Sample**	I_{814}^{lim}	**N**	**A**($I_{814}=21$)	**B**	**rms**
Cl0016+16	E+S0	<23	91	2.363(11)	−0.0673(99)	0.092
		<22	57	2.361(10)	−0.0677(144)	0.076
		<21	29	2.339(18)	−0.0941(220)	0.063
		<23	91	2.364	−0.0695	0.092
	E	<23	48	2.368(12)	−0.0605(126)	0.082
		<22	36	2.355(13)	−0.0857(167)	0.074
		<21	19	2.338(23)	−0.0981(248)	0.059
	S0	<23	15	2.358(22)	−0.0549(263)	0.080
Cl0054−27	E+S0	<23	30	2.270(18)	−0.0898(148)	0.091
		<22	21	2.252(21)	−0.1184(238)	0.081
		<23	30	2.265	−0.0695	0.096
Cl0412−65	E+S0	<23	20	2.289(31)	−0.0906(287)	0.131
		<23	20	2.290	−0.0695	0.137
All	E+S0	<23	141	2.333(10)	−0.0695(86)	0.108
		<22	93	2.337(10)	−0.0614(124)	0.091
		<21	54	2.342(18)	−0.0571(196)	0.081
	E	<23	65	2.357(10)	−0.0618(99)	0.082
		<22	48	2.350(12)	−0.0708(137)	0.076
		<21	27	2.347(21)	−0.0748(197)	0.058
	S0	<23	22	2.354(17)	−0.0558(214)	0.076
		<22	19	2.357(23)	−0.0468(366)	0.073

This figure "duv_fig1a.jpg" is available in "jpg" format from:

http://arXiv.org/ps/astro-ph/9607154v2

This figure "duv_fig1b.jpg" is available in "jpg" format from:

http://arXiv.org/ps/astro-ph/9607154v2

This figure "duv_fig1c.jpg" is available in "jpg" format from:

http://arXiv.org/ps/astro-ph/9607154v2